Cell

Intramolecular Strain Coordinates Kinesin Stepping Behavior along Microtubules

Ahmet Yildiz,[1] Michio Tomishige,[1,2] Arne Gennerich,[1] and Ronald D. Vale[1,*]
[1]Department of Cellular and Molecular Pharmacology and the Howard Hughes Medical Institute, University of California, San Francisco, CA 94158, USA
[2]Present address: Department of Applied Physics, University of Tokyo, 113-8656 Tokyo, Japan
*Correspondence: vale@cmp.ucsf.edu
DOI 10.1016/j.cell.2008.07.018

SUMMARY

Kinesin advances 8 nm along a microtubule per ATP hydrolyzed, but the mechanism responsible for coordinating the enzymatic cycles of kinesin's two identical motor domains remains unresolved. Here, we have tested whether such coordination is mediated by intramolecular tension generated by the "neck linkers," mechanical elements that span between the motor domains. When tension is reduced by extending the neck linkers with artificial peptides, the coupling between ATP hydrolysis and forward stepping is impaired and motor's velocity decreases as a consequence. However, speed recovers to nearly normal levels when external tension is applied by an optical trap. Remarkably, external load also induces bidirectional stepping of an immotile kinesin that lacks its mechanical element (neck linker) and fuel (ATP). Our results indicate that the kinesin motor domain senses and responds to strain in a manner that facilitates its plus-end-directed stepping and communication between its two motor domains.

INTRODUCTION

Kinesin 1 (herein referred to as kinesin) transports intracellular cargoes, such as membrane organelles, mRNAs, and protein complexes, along microtubules (Vale, 2003). Kinesin advances along its track in a remarkably precise manner. Each ATP binding/hydrolysis cycle causes kinesin to take an 8 nm step (Svoboda et al., 1993), the distance between adjacent α/β tubulin dimers along the long axis of the microtubule. At low loads, these steps are virtually always directed along a single protofilament track toward the microtubule plus end (Carter and Cross, 2005; Ray et al., 1993).

The mechanism of kinesin stepping along microtubules has been studied extensively. There is now general agreement that the two identical motor domains (also termed "heads") in the kinesin dimer move in a hand-over-hand manner, with the trailing head passing its stationary partner head and then attaching to the next available binding site on the microtubule (Asbury et al., 2003; Kaseda et al., 2003; Yildiz et al., 2004). The conformational change that drives this hand-over-hand motion has been proposed to be the "docking" of a ~14 aa peptide (the "neck linker") onto the catalytic core of the "front" head, which occurs upon binding of ATP (Rice et al., 1999). Since the C terminus of the docked neck linker is repositioned toward the microtubule plus end, this conformational change would be expected to shift the position of the "rear" head forward and bias its reattachment to the next available tubulin-binding site in the plus end direction. Although evidence for this conformational change has been obtained (Rosenfeld et al., 2001; Skiniotis et al., 2003; Tomishige et al., 2006), it still remains controversial whether the neck linker docking powers kinesin movement (Schief and Howard, 2001; Block, 2007; Carter and Cross, 2005).

How kinesin's two heads coordinate their ATPase cycles during processive movement also remains an important unresolved question in the motility mechanism. If the nucleotide- and microtubule-binding states of the two heads are completely unsynchronized, then kinesin would not be able to achieve tight chemomechanical coupling (each ATP hydrolysis leading to a step) and possibly its high processivity (Valentine and Gilbert, 2007). To coordinate the activities of the two heads and keep them out of phase, it is believed that a chemical or structural transition in one head is inhibited until the partner head proceeds through a critical step in its cycle (referred to as a "gating" mechanism).

Several theories have emerged as to how one kinesin head might wait for its partner (reviewed in Block, 2007; Hackney, 2007). "Chemical gating" mechanisms propose that either ATP binding to the nucleotide-free front head is inhibited until the rear head dissociates from the microtubule (Klumpp et al., 2004; Rosenfeld et al., 2003) or that ADP release from the trailing head is repressed until it is propelled to a forward position by ATP binding/neck linker docking in the front head (Crevel et al., 2004; Schief et al., 2004). Alternatively, kinesin might be gated through "tubulin binding." In such a mechanism, kinesin waits in a one-head-bound intermediate, and the detached "stepping" head cannot bind to the next tubulin-binding site until the partner head binds ATP (Alonso et al., 2007). Another general class of gating models proposes that the "detachment" of the rear head requires or is facilitated by tension generated from a "power

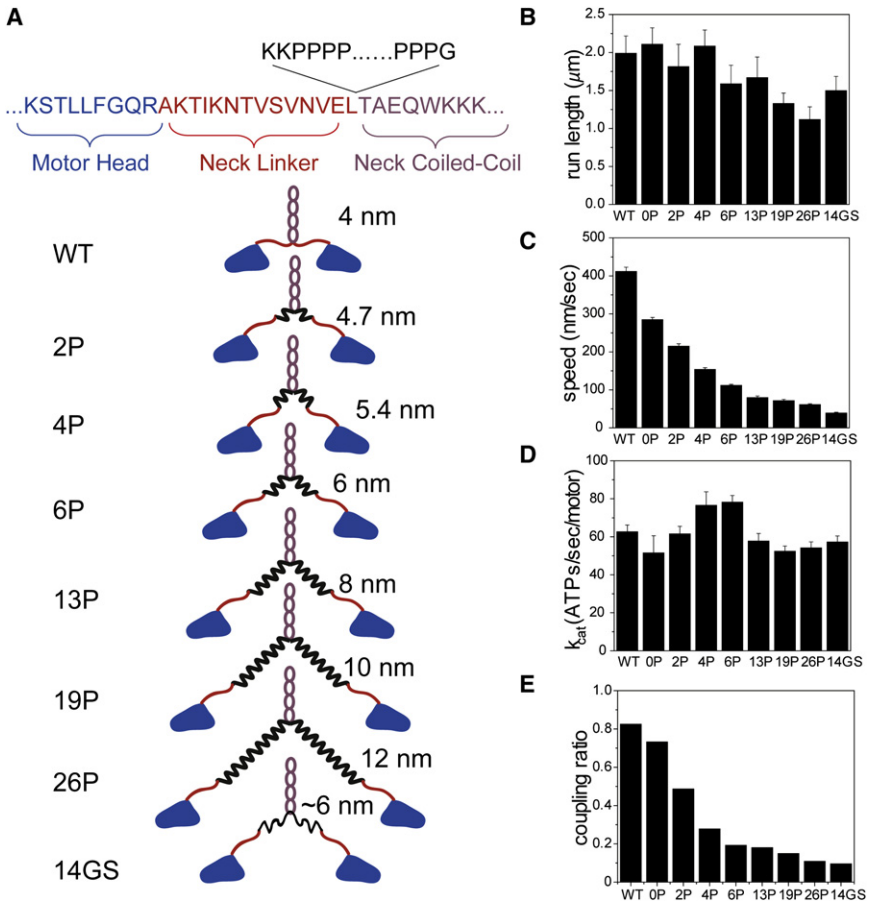

Figure 1. Motility Properties of Kinesins with Extended Neck Linkers

(A) Various lengths of polyproline and glycine-serine repeats, preceded by two lysines and followed by a single glycine residue, were inserted between the neck linker (red) and the neck coiled-coil domains (gray). As examples, insertions (black) of 2, 4, 6, 13, 19, 26 prolines (2P, 4P, 6P, 13P, 19P, and 26P) are expected to extend the neck linker length to 4.7, 5.4, 6, 8, 10, and 12 nm, respectively. The insert of seven repeats of glycine and serine (14GS) is depicted as a flexible 6 nm linker.

(B) and (C) Average run lengths and speeds of single GFP-tagged kinesin molecules at 1 mM ATP (mean ± SEM, N = 110–187).

(D) Maximum ATP turnover rates of GFP-tagged kinesin dimers are similar at saturating microtubule concentrations (mean ± SEM, N = 3 protein preparations).

(E) Calculated coupling ratio of mechanical stepping to ATP hydrolysis. See Supplemental Experimental Procedures for details of these calculations.

stroke" in the front head (Hancock and Howard, 1999; Spudich, 2006). These hypotheses are not mutually exclusive, and more than one gating strategy might be used by kinesin.

Resolving the structural basis of kinesin gating constitutes an additional challenge. In the microtubule-bound kinesin dimer, the neck linker in the front and rear head points backward and forward, respectively, and these different positions might regulate nucleotide- (Guydosh and Block, 2006; Tomishige et al., 2006; Uemura and Ishiwata, 2003) or microtubule-binding affinity (Kawaguchi and Ishiwata, 2001). Intramolecular strain might also be transmitted through the neck linkers when they are stretched to allow the two kinesin heads to bind simultaneously to the microtubule (Figure S1 available online). Evidence that the neck linker position or strain mediates kinesin gating is primarily based on differences in the ATPase properties of wild-type kinesin dimer and truncated kinesin monomers (Hancock and Howard, 1999; Rosenfeld et al., 2003), and certain point mutants (Klumpp et al., 2004); however, these reported changes in ATPase activity might be due to differences in the constructs rather than neck linker mediated strain.

In this study, we have explored the role of the neck linker in kinesin stepping and gating by engineering kinesin constructs with extended neck linkers designed to decrease mechanical tension between the motor domains (Hackney et al., 2003). These "extended" kinesins remain processive, but show a "gating" defect, reflected in a decrease in motor velocity due to impaired coupling of ATPase turnover to forward stepping. However, the velocity of movement can be increased by chemically cross-linking the neck linkers to partially restore intramolecular tension or applying external tension on the motor with an optical trap. We also show that external tension can initiate the stepping of a kinesin motor that lacks its mechanical element (the neck linker), as well as wild-type kinesin that lacks a chemical energy source (ATP). These results suggest that the dissociation of the rear kinesin head, promoted by tension from either neck linker docking in the front head or force produced by an optical trap, constitutes a "gate" that must open for kinesin to initiate its 8 nm step.

RESULTS

Engineering Kinesin Motors with "Extended" Neck Linkers

To test whether intramolecular tension plays a role in the kinesin mechanism, we attempted to reduce such tension by inserting additional residues between the neck linkers and the neck coiled-coil (Figure 1A). A similar strategy was used previously by Hackney et al. (2003), who inserted 6–12 additional residues between the neck linker and coiled-coil stalk and found that such extensions decreased kinesin's kinetic processivity (defined as the ATPs hydrolyzed per microtubule encounter). However, the motility of single kinesin motors was not examined in their study. Two types of insertions were used in this work (Figure 1A). The first insertion type consisted of polyproline of varying lengths (2P, 4P, 6P, 13P, 19P, and 26P, which form rigid helices with linear dimensions of 0.7, 1.4, 2, 4, 6, and 8 nm, respectively) (Schuler et al., 2005). The second was a disordered insert consisting of seven repeats of glycine-serine residues

(14GS), which increases the chain length of the random neck linker and effectively reduces the tension between the two heads (see Supplemental Text). Each insert was flanked by two added lysine residues at the N terminus (to compensate for the loss of electrostatic interactions between the positively charged neck coiled-coil and the negatively charged tubulin C terminus due to peptide insertion) (Thorn et al., 2000) and a single glycine residue on the C terminus (as a flexible joint between the rigid proline helix and the neck coiled-coil).

The movement of single GFP-tagged motors was visualized by total internal reflection fluorescence (TIRF) microscopy. Surprisingly, despite the dramatic changes to the neck linker, all of the extended kinesins moved processively, taking >100 steps along the microtubule without dissociating. The average run lengths were similar to wild-type kinesin (WT) (Figures 1B and S2). Even the longest insertion (26P) displayed a run length that was 60% of WT. These findings contrast with the results from prior ATPase studies by Hackney et al. (2003), which suggested that insertions to the neck region severely impair kinesin processivity. Thus, our direct single molecule measurements show that kinesin can maintain its high processivity even after diminishing the mechanical tension between its catalytic domains.

The extended kinesins, however, moved significantly slower than WT. The velocity of the proline insertion constructs decreased progressively with the number of inserted proline residues, with the longer inserts (13P, 19P, and 26P) moving at ~5-fold lower rates than WT (Figure 1C). The more flexible 14GS insertion resulted in an even greater decrease (10-fold lower than WT). Slow movement of the constructs was not due to impaired ATP hydrolysis, since the maximal MT-stimulated ATP turnover rates (k_{cat}) were similar between WT and the extended kinesins (Figure 1D). This result indicates that the extended kinesins are less efficient in converting ATP hydrolysis energy into productive unidirectional motion. An estimated coupling ratio (Figure 1E) revealed that WT kinesin is at least 80% efficient in converting ATPs hydrolyzed into forward steps, whereas the extended kinesins show a much lower coupling efficiency (as low as ~10% for the long extended kinesins).

The decreased velocity and chemomechanical coupling of the extended kinesins is most likely due to the loss of intramolecular tension, but it was important to rule out alternative consequences that might arise from neck linker amino acid insertion. We therefore investigated whether it might be possible to increase the velocity of an extended kinesin by restoring tension via chemical crosslinking. To accomplish this, we inserted a cysteine at the N terminus of the 13P insertion in a cysteine-light kinesin construct (termed Cys-13P) (Figure 2A) and then covalently linked these cysteines in the two chains of the kinesin dimer with a bifunctional crosslinking agent. The position of this interchain crosslink should be similar to the start of neck coiled-coil in WT kinesin and thus might be expected to restore intramolecular tension. Under optimized conditions, ~50% of the Cys-13P kinesin construct were crosslinked, whereas the cysteine-light kinesin template showed no crosslinking (Figure 2B). In the absence of crosslinker, Cys-13P moved at 116 nm/s (Figure 2C). However, in the presence of crosslinker, a second, higher velocity peak was observed at 250 nm/s (Figure 2D). The approximate proportion of these two peaks is consistent with the ratio of crosslinked to non-crosslinked motor (Figure 2B). These crosslinking experiments further support our conclusion that tension between the two heads is important for the normal velocity of kinesin movement.

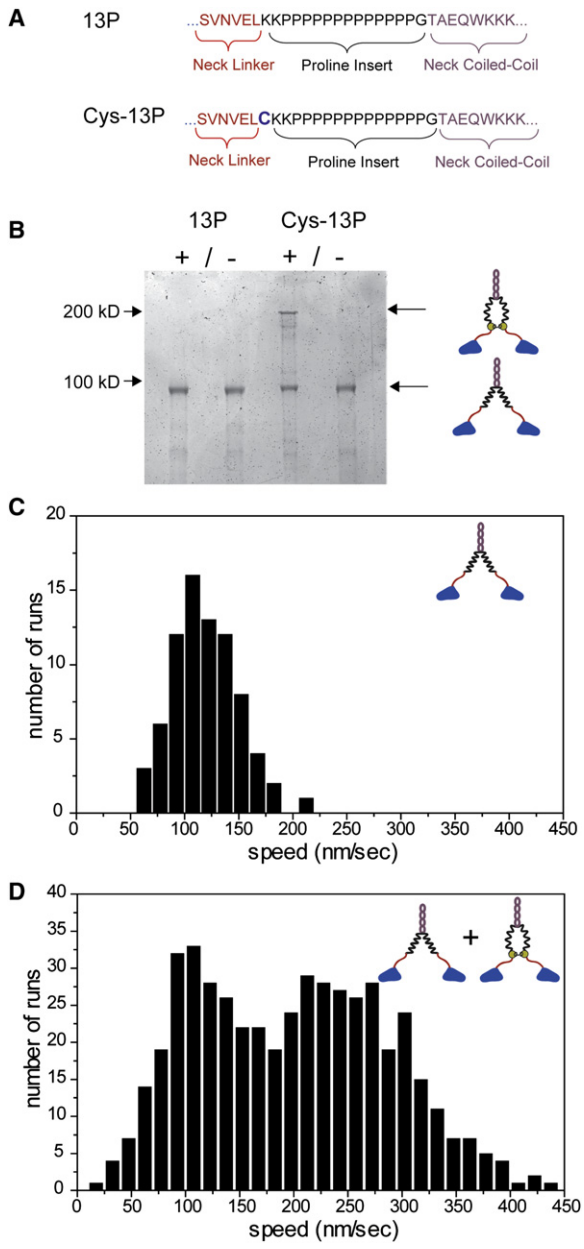

Figure 2. Chemical Crosslinking of the Neck Linker in an Extended Kinesin Increases the Velocity of Movement

(A) A unique cysteine residue was added to the N terminus of the 13P insertion in a cys-light kinesin construct.

(B) Specific interchain crosslinking of Cys-13P, but not 13P, induced by a bifunctional crosslinking agent (Coomassie stained SDS-PAGE gel).

(C) Speed histogram of single Cys-13P molecules without crosslinking shows a peak at 116 nm/s.

(D) After crosslinking, Cys-13P shows a second peak at higher speeds centered around 250 nm. The bimodal distribution of steps agrees with mixed populations of crosslinked and non-crosslinked kinesin observed in SDS-PAGE.

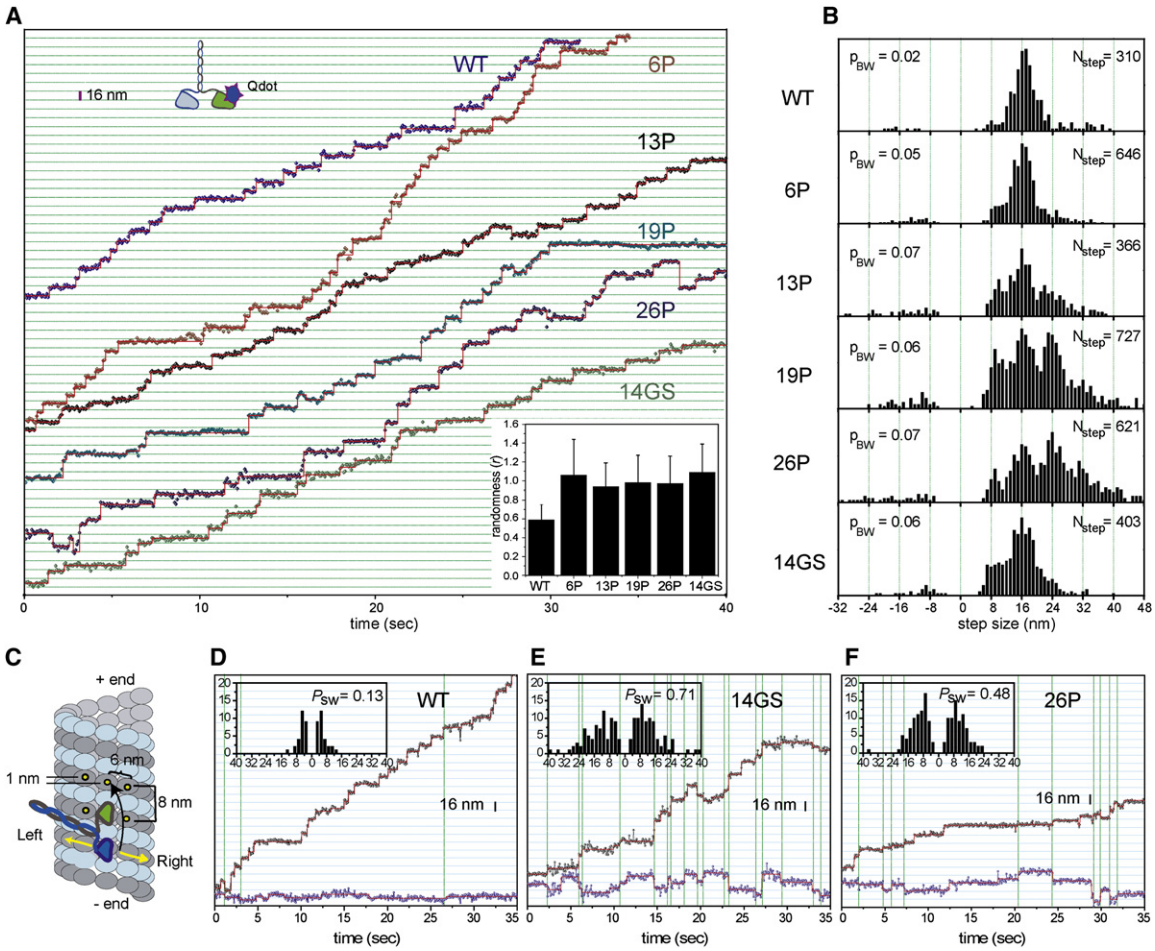

Figure 3. Stepping Behavior of Extended Kinesin Mutants

(A) Kinesin motors were labeled with a single quantum dot on one head, and head movement was recorded with 70 ms integration time. Stepping traces of WT (blue), 6P (wine), 13P (black), 19P (cyan), 26P (navy), and 14GS (olive), fitted with a step detection program (red lines) (Kerssemakers et al., 2006). Motor velocity was kept in the range of 10–15 nm/s by adding different concentrations of ATP for each construct (1 μM for WT, 15 μM for 6P and 13P, 25 μM for 19P, 40 μM for 26P, and 100 μM for 14GS) (see Experimental Procedures for details). The inset shows the randomness parameter (*r*) calculated from the dwell time measurements and suggests a coupling defect for extended kinesins (mean ± SD).

(B) A histogram of analyzed step sizes along the microtubule axis shows that the WT head moves with a consistent 16 nm step, whereas the head of the neck mutants takes highly variable steps that show peaks at multiples of ~8 nm. The number of analyzed steps (N_{step}) and probability for each construct to take a backward step (p_{BW}) are indicated in each panel.

(C) Available binding sites (black circles) for the rear head in the microtubule plus end direction.

(D), (E), and (F) Traces showing motor head displacement parallel (black trace) and perpendicular (blue trace) to the long microtubule axis for WT, 14GS, and 26P, respectively. Vertical dotted lines indicate diagonal steps. The inserts show histograms of sideways step sizes, separated into left and right directions. The overall probability of taking a sideways step (p_{sw}) is shown on each panel.

Extended Kinesins Take Highly Variable Steps

Kinesin moves along the microtubule with highly regular 8 nm steps, in contrast with such other motors as myosin VI (Rock et al., 2001) and dynein (Reck-Peterson et al., 2006), which take highly variable steps. Kinesin's center-of-mass step size may be restricted to 8 nm as a result of geometrical constrains. The dimensions of the two fully extended neck linkers in the dimer (~10 nm span) would allow the rear head to step to the next available tubulin dimer along the protofilament and not extend further forward or sideways. However, this hypothesis has not been tested directly. By extending the length of the neck linkers, we tested whether the motor can now take different sized steps. One head of the kinesin dimers was labeled with a single quantum dot, which provides a bright signal for high precision (1 nm) fluorescence tracking with better time resolution (70 ms) than in prior studies with fluorescent dyes (Yildiz et al., 2003).

The Q-dot-labeled WT kinesin head took regular 16 nm steps (Figures 3A and 3B), consistent with prior results and indicative of hand-over-hand movement of the heads (Yildiz et al., 2004). However, the steps taken by extended kinesins were often larger

and highly variable (Figures 3A, 3B, and S3). For example, 26P step size histogram showed a major peak at 24 nm as well as peaks at 8, 16, and 32 nm. For the very shortest insertions (0P, 2P, and 4P), the head step size was less variable and similar in size to that of WT kinesin (Figure S4). These results indicate that extending the reach of the kinesin dimer by elongating the neck linker with a rigid proline helix of sufficient length enables the rear head to move beyond the first available tubulin-binding site after it passes its partner head. The step sizes, however, were shorter than expected if the neck linker was predicted to be fully extended. For example, 13P (4 nm helix) approximately doubles the length of the native neck linker, but relatively few (~2%) steps were 32 nm in size and some were even shorter than 16 nm. This could be due to the flexible hinges on either side of the proline helix, which would prevent the entire linker region from fully extending in one dimension (Figure S5). The structure of the neck linker extension also affected motor stepping, since 14GS showed a distinct step size distribution, compared with 13P. In fact, the average step size of 14GS is lower than that of WT kinesin because of the appearance of ~8 nm steps (see discussion in Figure S5). A strong forward bias was still preserved, although the frequency of backward stepping was higher for extended kinesins (5%–7%) than for WT (<2%).

The neck linker insertions also affected the trajectory of kinesin stepping. Previous measurements showed that native kinesin follows a linear trajectory (Ray et al., 1993), even when subjected to a sideways load (Block et al., 2003). Examining an individual quantum dot-labeled head of WT kinesin in two dimensions, we find occasional (13%) ~6 nm sideways steps (with equal preference for right and left), most likely reflecting the movement of the head to a neighboring protofilament (Figures 3C and 3D). In contrast, heads of extended neck linker mutants took larger (4–20 nm) and more frequent (40%–70%) sideways as well as backward (~8 nm) steps (Figures 3B, 3E, and 3F). The majority (~70%) of lateral steps occurred simultaneously with a step along the microtubule axis (vertical lines in Figures 3D, 3E, and 3F), implying that the motor head can bind to sites in front or on either side as it moves forward. Taking into account the full step size in two dimensions did not significantly alter the step size distribution shown in Figure 3B (Figure S6). Interestingly, the lateral steps of 26P were significantly shorter (12.5 nm average) than the steps along the microtubule axis (21.5 nm), suggesting that the motor is still biased to move forward, rather than completely free to diffuse around its tether.

In summary, changing the length and mechanical properties of the neck linker dramatically alters the stepping behavior of kinesin, while still retaining the motor's ability to move processively along the microtubule.

Extended Kinesins Undergo Futile Cycles of ATP Hydrolysis

The ATPase and velocity data described above suggested that extended kinesins undergo "futile" ATPase cycles, hydrolysis events that do not lead to forward movement. We searched for additional evidence of such uncoupling by performing a fluctuation analysis of dwell times in between steps, which yields a randomness parameter, "*r*" (Schnitzer and Block, 1997) (Supplemental Text). An *r* value of 0 reflects a constant dwell time between steps, whereas *r* values of 1 and 0.5 are expected for motors with one and two rate-limiting transitions per step, respectively. Our dwell time analysis of WT kinesin (one head labeled) at low ATP revealed an *r* of 0.57 (Figure 3A, inset), reflecting the expected two successive ATP-binding events that occur between 16 nm steps (the head takes a 16 nm step during one ATP binding or turnover, but remains stationary during the next cycle while its partner head is moving). In contrast, the extended kinesins showed larger fluctuations of their dwell times (r = 0.97–1.01), which is most likely caused by a lower stepping probability per ATP-binding event (Schnitzer and Block, 1995). These data indicate that extended kinesin motors often fail to step forward after binding or hydrolyzing ATP, in contrast to WT kinesin. In addition, a histogram of WT kinesin dwell periods can be fit well to a convolution of two exponentials, as expected from a tight coupling of ATP binding to hand-over-hand movement of the heads (Yildiz et al., 2004). However, extended kinesins display an additional population of very long dwells, which likely reflects impaired coupling of ATP hydrolysis to a mechanical step (Figure S7).

The Velocity of Extended Kinesin Movement Can Be "Rescued" by an Assisting Load

The response of the extended kinesins to external loads was examined using an optical trap assay in which single GFP-tagged kinesin motors were coupled to 1 μm beads via an anti-GFP antibody (see Experimental Procedures). In a fixed trap assay, extended kinesins stalled at lower opposing forces (~2–3 pN) than WT kinesin (7 pN) (Figure 4A). The lower force production of the extended kinesins indicates that tight mechanical coupling between the two heads can be important for the high stall force of WT kinesin (see discussion in Supplemental Text).

We then tested whether "external" tension from the optical trap might substitute for the loss of "internal" tension in the extended kinesin mutants, and thus restore chemomechanical coupling. Using a force-clamp optical trap (Gennerich et al., 2007), a constant 3, 6, or 9 pN assisting load was applied toward the microtubule plus end, kinesin's normal direction of travel. Because of the geometry of the experiment (diagram, Figure 4B), the applied load is primarily "felt" by the trailing head. For WT kinesin under a forward load of up to 9 pN, the velocity of movement remained largely unchanged (Figure 4C), as reported elsewhere (Block et al., 2003). If the extended kinesins move slowly under unloaded conditions because they cannot effectively detach the trailing head and pull it forward, we reasoned that the assisting load might increase their velocity of movement. Indeed, assisting loads dramatically increased the velocity of extended kinesins by several fold at 1 mM ATP. Inspection of the traces revealed that motion occurred in a step-wise manner (inserts in Figure 4B; step size analysis at lower ATP concentrations in Figure S8). At 6 pN forward load, the velocity of 13P, 14GS, and 26P approached that of WT kinesin, and at 9 pN, the extended kinesin constructs moved even faster than WT (Figure 4C). The higher velocities might be explained by the ability of extended kinesins to take larger steps. With the relatively low Brownian noise at 9 pN load, we could measure the

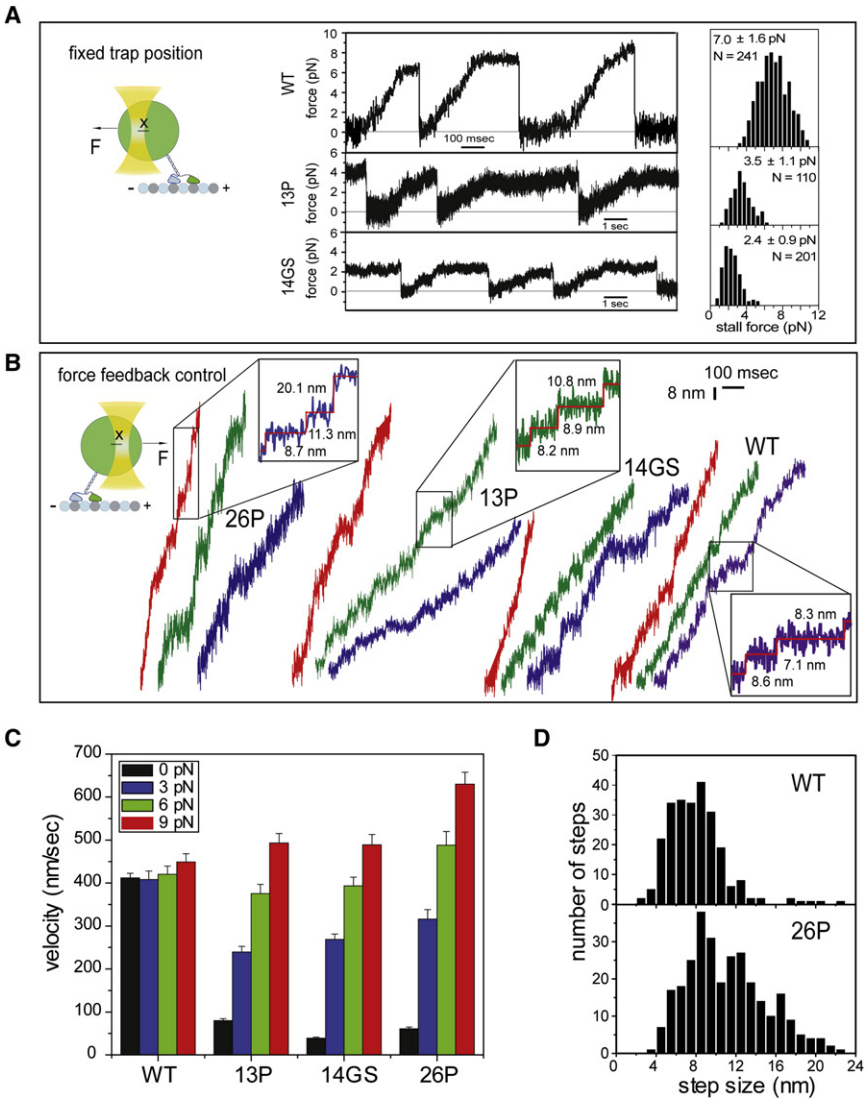

Figure 4. Extended Kinesin Velocity Can Be Rescued by an Assisting Load

(A) Schematic representation of a kinesin motor attached to a bead (green, not to scale) and trapped with a stationary laser beam (yellow), shown on the left. Displacement records of WT, 13P, and 14GS kinesin motors at 1 mM ATP show successive runs, stalling, and motor detachment events. The stall force distributions (mean ± SD, N = 100–300) are shown on the right.

(B) Kinesin movement under a constant assisting load applied by a force-feedback controlled trap (diagram). Individual traces of WT, 13P, 14GS, and 26P under 3 pN (blue), 6 pN (green) and 9 pN (red) forward load at 1 mM ATP show stepwise movement (inserts).

(C) Under forward load, the velocity of WT shows a very small increase, while 13P, 14GS, and 26P mutants speed up considerably with increasing load (mean ± SEM, N = 35–60).

(D) Histograms of center-of-mass steps at a 9 pN assisting load show a larger average step size for 26P (11.51 ± 4.89 nm [mean ± SD], N = 305) than WT (7.98 ± 2.89 nm, N = 250).

center-of-mass step sizes (expected to be half as large as the displacement of individual kinesin heads shown in Figure 3) for 26P and WT kinesin at saturating ATP (Figure S9). Figure 4D shows that 26P takes >8 nm steps with a 9 pN assisting load and thus its average step size (11.51 nm) is larger than that of WT kinesin (7.98 nm). We also found no clear backward steps (of 302 steps scored) at this assisting load. From these data, we calculated stepping rates for WT (56.2 s^{-1}: 449 nm/s velocity divided by a 7.98 nm step) and 26P kinesin (54.73 s^{-1}: 630 nm/s velocity divided by an 11.51 nm step). These similar stepping rates reveal that the 9 pN forward load rescues the coupling deficiency of the 26P extended kinesin.

We also examined force-assisted movement at low ATP concentrations. The extended kinesins normally did not show processive movement at <2 μM ATP, in contrast to WT kinesin, which moves at 100 nM ATP. However, with an assisting load, 14GS took progressive steps at 1 μM ATP (Figure S10). Collectively, these experiments demonstrate that intramolecular tension is critical for coordinating the alternating movements of kinesin's two motor domains and that external load can rescue the velocity defect caused by inserting amino acids after the neck linker.

ATP-Independent Kinesin Movement under Load

The finding that external load can rescue the velocity of the extended kinesins led us to further explore how the two heads in WT kinesin communicate with one another. We sought to test the idea that an ATP-induced neck linker docking in the leading kinesin head generates intramolecular strain that accelerates the dissociation rate of the trailing head and also provides the bias for the detached head to step forward. If this model is correct, then an externally applied load to the rear head might substitute for the action of neck linker, triggering repetitive stepping without ATP or even in the absence of the neck linker itself.

To test whether an external "load" might mimic the directional forces of a kinesin "power stroke," we pulled WT kinesin either toward the plus or minus end of the microtubule in different nucleotide conditions. Remarkably, in the complete absence of ATP, a constant load of 3 or 6 pN induced movement of WT kinesin either toward the plus or minus end of the microtubule (Figure 5A). This movement was clearly not due to nonspecific "slipping," since movement occurred in step-wise, ~8 nm center-of-mass displacements, even when applying two-dimensional loads (3 pN perpendicular and 6 pN parallel to microtubule axis) (data not shown). Under two dimensional forces, the bead would detach completely from the microtubule and move rapidly back to the trap center, if load-induced movement was due to complete unbinding and rebinding of kinesin. ATP-independent

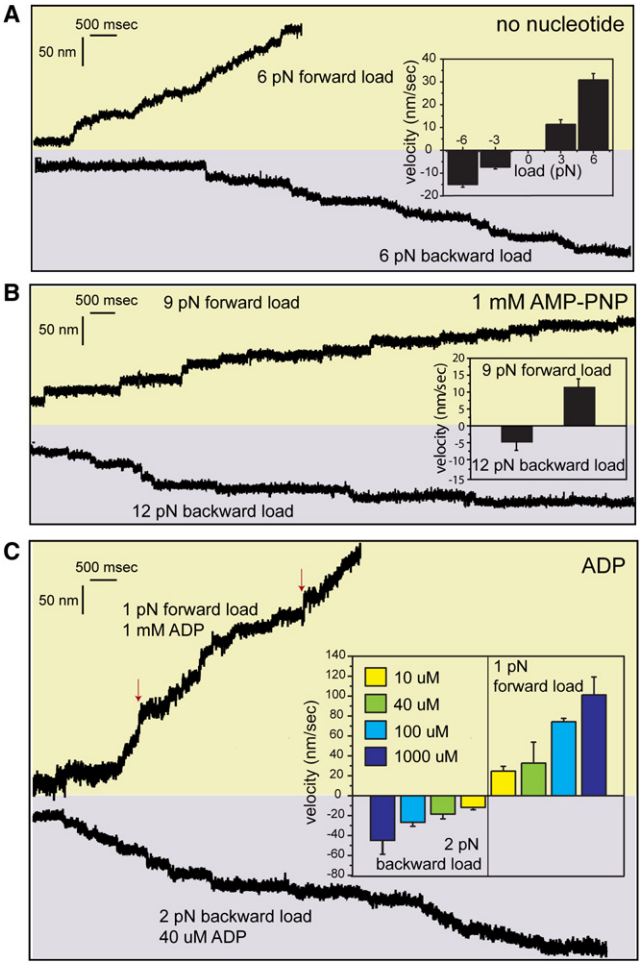

Figure 5. Load-Induced Kinesin Movement under Different Nucleotide Conditions

(A) In the absence of a nucleotide, WT kinesin motors displayed bidirectional movement under a 6 pN forward (plus-end-directed) or backward load. Motors moved faster toward the plus end under 6 pN load (30.8 ± 2.8 nm/s), compared with 3 pN load (11.3 ± 2.1 nm/s). Under 6 pN, higher velocities were recorded toward the plus end, compared with the minus end (8.5 ± 1.3 nm/s).

(B) In the presence of 1 mM AMP-PNP, higher loads were required to induce stepping of single kinesin motors. Under 9 pN forward load, WT kinesin took 8 nm center-of-mass steps along the microtubule with a velocity of 12 nm/s. 12 pN backward load was required to induce efficient movement at 5 nm/s.

(C) In the presence of ADP, kinesin displayed bidirectional movement along microtubules under forces as low as 1 pN in forward or 2 pN in backward direction. The inset shows the average velocities recorded at different ADP concentrations. The red arrows show a rare slippage (<3% of stepping) along the microtubule axis during processive movement. Mean and standard error of the mean are shown (N = 15–30 for each nucleotide condition).

stepping under tension was not expected, since a previous study reported that the rate of force-induced backward stepping of kinesin depends on the ATP concentration and concluded that backward as well as forward stepping required ATP binding (Carter and Cross, 2005). However, the Carter and Cross study did not directly test whether kinesin steps under nucleotide-free conditions under load. We also note that nucleotide-independent processive motion of kinesin was not reported by the unbinding force measurements of Uemura and Ishiwata (2003), which might be due to a nonconstant force (~5 pN/s loading rate) applied in their continuously moving trap. However, with a constant force applied in our feedback-controlled system, we conclude that force alone can induce an 8 nm step by promoting the detachment of the rear head and shifting its position forward past the bound head.

We also observed an inherent asymmetry in the force-induced movement, with faster velocities observed for an equal magnitude pull directed toward the microtubule plus end, compared with the minus end (Figure 5A). This result is consistent with the lower unbinding forces measured when kinesin is pulled toward the plus end, compared with the minus end (Uemura and Ishiwata, 2003) (see Discussion).

We next tested whether an applied force can induce movement in the presence of AMPPNP (a nonhydrolyzable ATP analog), which causes kinesin to bind more tightly to microtubules than in nucleotide-free conditions (Kawaguchi and Ishiwata, 2001), and ADP, which induces a weak binding state. With 1 mM AMPPNP, a 9 pN force was required to induce stepping toward the plus end, whereas higher forces of 12 pN were required to produce minus-end-directed stepping (Figure 5B). A 6 pN load, which induced stepping under nucleotide-free conditions, did not lead to stepping with 1 mM AMPPNP (Figure S11). In the presence of ADP, much lower forces of ~1 pN were sufficient to move kinesin toward the plus end (see Experimental Procedures) (Figure 5C). The velocity of movement was dependent on the ADP concentration (Figure 5C, insert), which likely reflects the relative time that the microtubule-bound kinesin head spends in a nucleotide-free state (resistant to detachment with a 1 pN load) versus a weakly bound ADP state (see also Uemura and Ishiwata, 2003). Once again, a higher load (2 pN) was required to drive the movement toward the minus end in the presence of ADP. In contrast to Uemura and Ishiwata (2003), we found that lower forces (1–2 pN) are sufficient to allow head detachment with bound ADP, compared with their reported average unbinding forces of 3–4 pN. The higher force measured by Uemura and Ishiwata is likely explained by their use of a constantly moving trap (instead of a force-feedback trap), which leads to a rapidly increasing load and the measurement of larger forces (depending on the time constant of detachment). In summary, these experiments reveal that the amount of force required for stepping is most likely determined by the affinity of the rear kinesin head for the microtubule. In addition, there is a clear directional asymmetry for detachment under all nucleotide conditions, with less force required for trailing head detachment when the pull is in the normal direction of kinesin movement.

We next explored whether a pulling force might substitute for a force-inducing conformational change of the neck linker. To test this idea, we deleted the native neck linker sequence that docks onto the catalytic core and added 19 prolines to act as a spacer between the catalytic core and coiled-coil (19P-NL) (Figure 6A). This construct displayed no detectable movement in single-molecule assays with 1 mM ATP (Figure 6B). Remarkably, an external force (3 or 6 pN) from the optical trap caused the "immotile" 19P-NL mutant to step along the microtubule (Figure 6C) with a similar rate to that of WT in the absence of

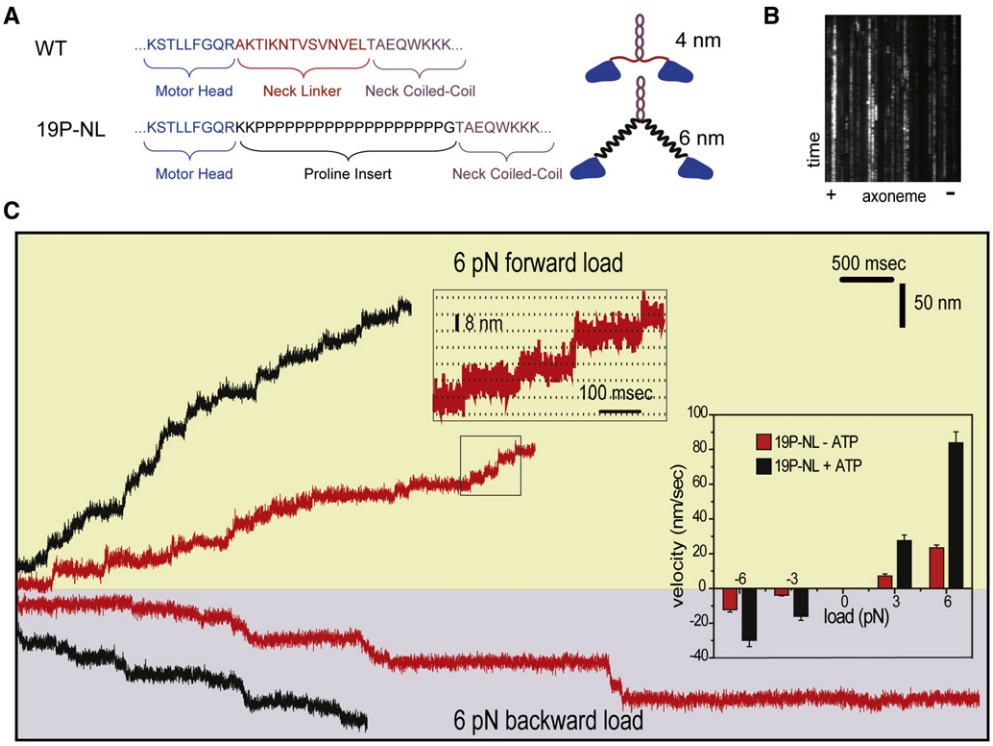

Figure 6. Role of Neck Linker in Kinesin Stepping

(A) Kinesin's native neck linker sequence was replaced by 19 proline residues (19P-NL).

(B) A kymograph shows that the fluorescently tagged 19P-NL construct does not move along axonemes with 1 mM ATP.

(C) Under 6 pN external load, 19P-NL showed processive movement in both directions. The insert shows that the force-induced kinesin movement occurs by consecutive 8 nm displacements and not by slippages along the microtubule axis. The motor moved faster under 1 mM ATP (black traces), compared with no nucleotide condition (red traces). Bar graph shows the measured velocities (mean ± SEM, N = 40–70).

ATP. Load-induced movement in the presence of 1 mM ATP for 19P-NL was ~4-fold faster (84 ± 6 nm/s) than that under nucleotide-free conditions. Although immotile, 19P-NL has ATPase activity (5-fold lower than WT), which enables its trailing head to transit from a tight (nucleotide-free) to a weak (ADP) binding state. As described above, the ADP state is more susceptible to detachment under load, which most likely accounts for the higher velocities of 19-NL in the presence of ATP. In summary, these results show a kinesin lacking its mechanical element and ATP, can undergo 8 nm unidirectional stepping, if external tension is applied to the motor.

DISCUSSION

By modulating the length of kinesin's neck linker and performing single molecule analysis, we have obtained several results that provide new insights into the role of this mechanical element in kinesin motility. First, kinesin can tolerate dramatic alterations in the size and structure of the mechanical elements that interconnect the two motor domains and still move processively along the microtubule. However, these structural perturbations are not without consequence. Extended kinesins now reach farther with their elongated neck linkers, frequently taking larger as well as sideway steps, similar to cytoplasmic dynein (Reck-Peterson et al., 2006). The most prominent "loss of function" of the extended kinesins is their slow velocity due to impaired chemomechanical coupling, a defect that is most readily explained by the loss of intramolecular tension. This interpretation gains support from the finding that velocity of an extended kinesin can be recovered to nearly wild-type levels either by chemically crosslinking the two kinesin polypeptide chains at the end of the native neck linker or by generating tension on the trailing head with an optical trap. External load also can cause kinesin to step forward or backward in the absence of ATP or without its neck linker. These results also were unexpected, since previous studies have concluded that ATP binding is necessary for both forward as well as backward kinesin stepping (Carter and Cross, 2005, 2006). Collectively, our work provides new insight into the structural basis of kinesin stepping, tension sensing by the kinesin motor domain, and how the two kinesin heads coordinate their activities during processive motion, as discussed below.

A Model for Communication between the Two Kinesin Heads

Models for the communication between the two kinesin heads are quite varied and a topic of considerable debate. A role of intramolecular tension between the two kinesin heads in head-head communication was first evoked by Hancock and Howard (1999) on the basis of their data showing that truncated monomeric kinesins displayed 10-fold lower microtubule-stimulated

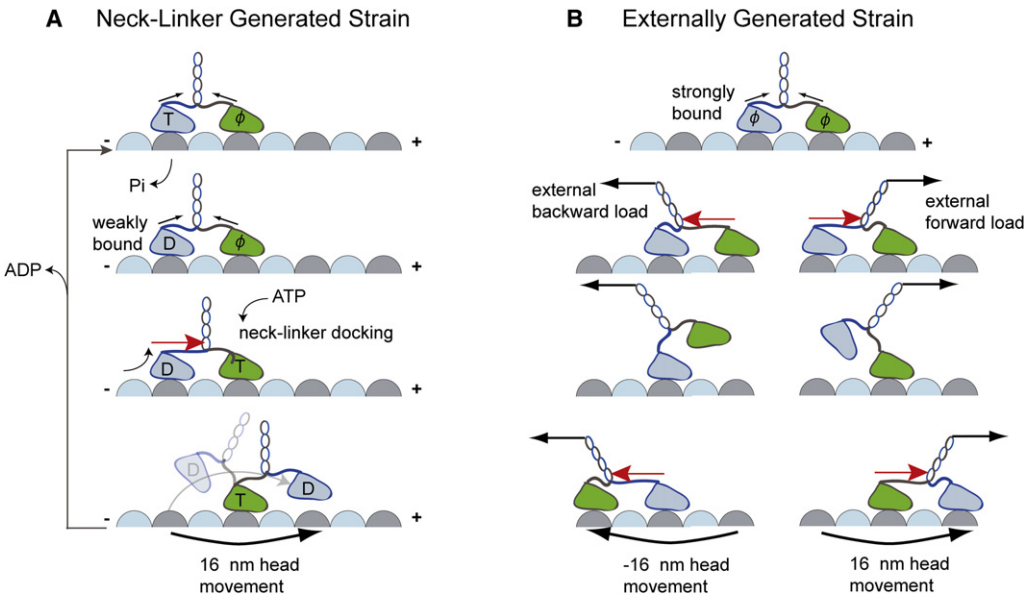

Figure 7. Internal or External Strain Facilitates Kinesin Stepping

(A) Model for ATP-dependent kinesin stepping by neck linker–generated strain. ATP binding to the front head causes neck linker docking, which increases intramolecular strain (red arrow); forward strain on the rear head favors its dissociation after it transits to a weakly bound ADP state (panel D). After its dissociation, the head shifts forward, biasing its attachment to the next available forward binding site. Note, however, that intramolecular strain from the stretched neck linkers (Figure S1) may suffice to release the rear head in its ADP state, without neck linker docking.

(B) Strain on kinesin heads can be generated by external load (black arrows). Forward load increases the strain on the rear head by pulling the neck linker. This favors the rear head detachment and displacement toward the microtubule plus end (right). Similarly, a backward load pulls the front head backward as a result of strain-dependent detachment (left). This type of stepping can occur in the absence of ATP and the neck linker.

ATPase and microtubule dissociation rates than dimeric kinesin. However, this result was not confirmed in other studies (e.g., Rosenfeld et al., 2003). Recent studies have postulated that kinesin waits for a step with only one-head bound, in which case interhead strain is not present and an alternative gating mechanism must be evoked (Carter and Cross, 2005; Alonso et al., 2007). Thus, whether intramolecular tension is important for the kinesin mechanism is controversial and not resolved by a direct experiment. The experiments described here showing the increase in velocity of extended kinesins by applying external tension or interchain crosslinking arguably provide the most direct evidence to date for a role of tension sensing in the head-head coordination during motility.

How might intramolecular tension facilitate kinesin walking? Our results suggest that tension regulates microtubule dissociation of the rear kinesin head (Figure 7). In the absence of ATP (a condition where chemical gating is not possible), kinesin will step forward or backward if pulled upon by an optical trap. Under an assisting load, the tension is experienced primarily by the trailing head, causing it to release, shift forward, and then rebind along the microtubule. These events can happen repeatedly, and the motor can walk processively along the track. A similar phenomenon has been observed for cytoplasmic dynein (Gennerich et al., 2007) and myosin V (Gebhardt et al., 2006), suggesting that force-induced detachment might be a general design plan of molecular motors.

We also show that nucleotide-free walking can occur without the native neck linker, suggesting that the sensor for tension-induced detachment resides within the microtubule interface of the kinesin motor domain itself. This interface also has an asymmetry for force-induced dissociation, with preferential release with a plus-end-directed force (our data and Uemura and Ishiwata, 2003). Thus, intramolecular tension would favor the release of the rear head, helping to maintain head-head coordination and processivity.

Synthesizing these results and work of others, we suggest a model for how kinesin heads communicate during motility (Figure 7). For kinesin to take an 8 nm step, two events have to happen: 1) the rear head has to detach, and 2) the neck linker has to dock to pull the detached head forward. The finding that external tension promotes rear head detachment leads us to propose that intramolecular strain promotes rear head dissociation. Moreover, strain-mediated rear head detachment is likely synchronized with its nucleotide state. If the rear head is in an ATP or ADP-Pi state, then our results suggest that large forces (~9 pN; Figure 5) are required to dissociate the head, which may likely exceed the forces produced by intramolecular tension. However, after the rear head releases the inorganic phosphate and is in a weak-binding ADP state, then lower forces (~1 pN) would suffice for rear head detachment. Such a mechanism also would allow kinesin to synchronize the timing of its step with distinct chemical states in the front and rear heads. To enable rapid rates of kinesin stepping at saturating ATP concentrations, we also propose that the partial docking of the neck linker in the front head upon ATP binding accelerates rear head release (by providing a directional force that increases the tension on the

rear head, similar to the assisting pull from an optical trap; Figure 7). However, further experiments will be required to determine whether neck linker docking can be initiated in the front head prior to rear head release and the magnitude of added tension that might be produced (discussed below).

This model does not preclude a "chemical gate," which surely must also exist. Early kinetic experiments (Gilbert et al., 1998; Hackney, 1994) showed that ADP release of one head was greatly accelerated by ATP binding to the partner head on the microtubule. However, the lack of ADP release in one head may not be simply explained by that head not being able to access the microtubule (Hackney, 2005). In addition, compelling experiments by Guydosh and Block (2006) showed that kinesin must first take a backward step to escape from a block created by the binding of a nonhydrolyzable nucleotide to one of the kinesin heads. The result was interpreted as evidence for strain-regulated nucleotide binding to the front head. However, the Guydosh and Block results can also be interpreted as nucleotide release from the rear head being inhibited, perhaps due to forward pointing position of the neck linker (Mori et al., 2007).

A chemical gate of kinesin could operate in concert with strain-dependent dissociation of the rear head from neck linker docking. However, a rear head detachment mechanism that is promoted by neck linking docking (depicted in Figure 7) cannot operate with a chemical gate in which the front head cannot bind ATP until the rear head detaches. Further experiments will be needed to determine definitively which mechanism is operational in a walking kinesin motor. Another point that remains to be addressed is whether strain-dependent release operates at very low ATP concentrations. Our experiments show that external strain can increase the velocities of extended and WT kinesin at subsaturating ATP concentrations. Recent work by Mori et al. (2007) demonstrates a "one-head-bound" state of kinesin at low ATP concentrations, with the weak binding head positioned behind the strongly bound head. The rear head may still bind weakly to microtubules and be subject to complete detachment by force. Thus, it is possible that the force-induced velocity increase at low ATP concentrations occurs by either promoting rear head release or preventing reattachment of the detached head to the rear tubulin-binding site. Further insight into chemical gating also might be gained by understanding how ATP turnover becomes uncoupled from mechanical stepping in the extended kinesins. Such uncoupling might arise from ADP/ATP exchange in the rear head without its associated forward movement due to its "relaxed" neck linker. However, other mechanisms also could account for uncoupling, and new assays will be needed to probe the chemical cycle of kinesin at a single-molecule level.

The Role of the Neck Linker in Kinesin Stepping

Rice et al. (1999) originally proposed that ATP-induced neck linker docking in the front kinesin head triggers the 16 nm displacement of the rear head. However, a criticism of the neck linker theory is whether the docking of this small peptide to the catalytic core provides sufficient energy to power kinesin movement under load (Rice et al., 2003; Schief and Howard, 2001), although recent computational modeling suggests that additional energy may be derived through an interaction between the kinesin N-terminal peptide interacting with C-terminal neck linker in the ATP state (Hwang et al., 2008). Here, we show that kinesin without its neck linker will still walk processively if a "bias" is provided by an optical trap. This result reveals that, in the absence of a mechanical element, the motor domain responds to tension by releasing and rebinding to the microtubule. This result also implies that a key function of the neck linker and its ATP-driven conformational change is to provide a directional force that releases and biases the motor domain (which the trap can mimic in the 19P-NL experiment). As described above, a very small force may be needed to detach the rear head and bias its movement forward, whereas most of the energy needed to move kinesin forward against a 5–6 pN backward load would be derived from the subsequent reformation of tight kinesin-microtubule-binding interaction, which locks the step in place.

The 8 nm regular stepping of kinesin differs substantially from the cytoplasmic dynein motor, which takes a wide range of forward (4–24 nm), backward (20%), as well as sideways steps (Reck-Peterson et al., 2006; Gennerich et al., 2007). However, by extending the kinesin neck linker, we were able to produce a motor with a stepping behavior that is more similar to dynein than to WT kinesin. This result reveals that the regular pattern of stepping can be modulated by varying the length and flexibility of the elements interconnecting the two motor domains. In some cases, it may be advantageous to design highly efficient and regular motors (kinesin and myosin V), whereas in other cases, reducing motor efficiency but increasing its ability to move around the track (dynein and myosin VI) may help to avoid obstacles (Dixit et al., 2008). It will be interesting to explore how modulating a motor's stepping behavior affects its ability to execute transport functions in living cells.

EXPERIMENTAL PROCEDURES

Single Molecule Fluorescence Motility Assays

The construct design is described in the Supplemental Experimental Procedures.

For single-molecule motility assays, sea urchin axonemes were immobilized on a glass surface, and 200 pM kinesin motor was then perfused into the chamber in motility buffer (12 mM PIPES [pH 6.8], 1 mM $MgCl_2$, 2 mM EGTA, and 1 mg/ml casein) containing 2 mM DTT, 2% glucose, and 3 μl "gloxy" to remove free oxygen in solution (Yildiz et al., 2003). Speed and run length measurements were performed with GFP-labeled motors at 1 mM ATP using total internal reflection fluorescence microscopy, as described elsewhere (Reck-Peterson et al., 2006).

For high-precision fluorescent tracking, a unique reactive cysteine was introduced in the catalytic core (E215C), dialyzed motors were labeled with biotin-maleimide (EZ-link PEO_2, Pierce) at 0.5 biotins per head (2 hr, 4°C), the reaction was quenched with 2 mM DTT, and excess of biotin was removed through microtubule affinity purification. Microtubule-bound, biotinylated kinesin motors were incubated with 400 nM streptavidin-coated quantum dots (655 nm, Invitrogen) for 5 min within the flow chamber in the absence of ATP (reaction was performed on microtubule-bound kinesin to avoid aggregation from multivalent quantum dots). The sample was washed with imaging buffer containing 140 mM 2-mercaptoethanol. Motor velocity was kept in the range of 10–15 nm/s by adding different concentrations of ATP for each construct (see Figure 3 legend). At this speed, we could minimize scoring two successive steps as one "large step," since the motor's average dwell time (950 ms) was long, compared with the temporal resolution (70 ms). Our step detection program scores a dwell period consisting of three data points

(210 ms). At this time resolution, we estimate that only 2% of our scored steps will be due to the rapid succession of two steps. We also compared stepping of different constructs at similar average dwell times to minimize artifacts (such as selectively scoring two steps as one large step for one construct).

To crosslink the C termini of the neck-linker region, a cysteine was introduced to position 337 of the 13P cysteine-free mutant (Cys-13P). Purified Cys-13P (2 μM) were treated with 2 mM TCEP for 30 min and then were passed through a desalting column (NAP5, GE Healthcare), and a bifunctional maleimide crosslinker (BMOE, Pierce) was added at an equimolar ratio to motor for 4 hr in 80 mM Pipes (pH 7.0), 100 mM NaCl, 1 mM $MgCl_2$, and 1 mM EGTA at 4°C. The remaining crosslinker was quenched with 10 mM DTT for 30 min.

Optical Trapping Assays

Optical trap measurements of eGFP-tagged WT, 13P, 19P, and 14GS constructs were performed with a custom-built optical trapping microscope (Gennerich et al., 2007). Briefly, 0.92 μm diameter latex beads were crosslinked to anti-GFP antibodies and incubated with the GFP-tagged motors. The motor-bead ratio was adjusted so that 30% of the beads displayed movement. Under these conditions, there is >99% probability that bead movements were due to single kinesin molecules (Svoboda and Block, 1994). Spring constants of 0.04–0.06 pN/nm were used for WT to allow a maximal bead-trap separation of 100–150 nm. For the neck mutants, spring constants of 0.025–0.035 pN/nm were used.

Stall force measurements were performed with a fixed position optical trap. Kinesin stepping under constant loads was analyzed by using the force-feedback mode of the optical trap. Velocities were obtained by line fits to the displacement traces of the beads moving under constant load. Measurements in the absence of ATP were performed by adding 20 U/ml apyrase to deplete residual ATP and ADP (which would in any event be <3 nM after the final dilution of kinesin in the single molecule assay). Beads that bound to the axoneme (determined by the decrease in Brownian noise) did not show movement when the optical trap was turned off, confirming ATP depletion. Longitudinal forward and backward forces in the absence of ATP were applied to the motor via the force-feedback controlled trap (Supplemental Data). After completing the measurements of force-induced kinesin stepping in the absence of ATP, motor-bead solution containing 1 mM ATP was flown into the chamber to determine the polarity of the axoneme via kinesin-driven microtubule plus-end-directed bead movement. Pulling experiments in various concentrations of ADP were performed by adding 2U/ml hexokinase to ensure that movement was not induced by residual ATP in solution.

Analysis of steps and dwell times for both optical trap and single molecule fluorescence data was performed using the automated step-finding algorithm of Kerssemakers et al. (2006).

SUPPLEMENTAL DATA

Supplemental data include Supplemental Experimental Procedures, Supplemental Text, and eleven figures and can be found with this article online at http://www.cell.com/cgi/content/full/134/6/1030/DC1/.

ACKNOWLEDGMENTS

The authors thank A.P. Carter and N. Zhang for their help with protein purification and cloning and J. Kerssemakers and M. Dogterom for supplying their step finding algorithm. This work has been supported by Jane Coffin Childs Memorial Fund (A.Y. and A.G.), Burroughs Wellcome Fund (A.Y.), German Research Foundation (GE 1609/1 [A.G.]), and the Howard Hughes Medical Institute.

Received: March 3, 2008
Revised: May 28, 2008
Accepted: July 14, 2008
Published: September 18, 2008

REFERENCES

Alonso, M.C., Drummond, D.R., Kain, S., Hoeng, J., Amos, L., and Cross, R.A. (2007). An ATP gate controls tubulin binding by the tethered head of kinesin-1. Science *316*, 120–123.

Asbury, C.L., Fehr, A.N., and Block, S.M. (2003). Kinesin moves by an asymmetric hand-over-hand mechanism. Science *302*, 2130–2134.

Block, S.M. (2007). Kinesin motor mechanics: binding, stepping, tracking, gating, and limping. Biophys. J. *92*, 2986–2995.

Block, S.M., Asbury, C.L., Shaevitz, J.W., and Lang, M.J. (2003). Probing the kinesin reaction cycle with a 2D optical force clamp. Proc. Natl. Acad. Sci. USA *100*, 2351–2356.

Carter, N.J., and Cross, R.A. (2005). Mechanics of the kinesin step. Nature *435*, 308–312.

Carter, N.J., and Cross, R.A. (2006). Kinesin's moonwalk. Curr. Opin. Cell Biol. *18*, 61–67.

Crevel, I.M., Nyitrai, M., Alonso, M.C., Weiss, S., Geeves, M.A., and Cross, R.A. (2004). What kinesin does at roadblocks: the coordination mechanism for molecular walking. EMBO J. *23*, 23–32.

Dixit, R., Ross, J.L., Goldman, Y.E., and Holzbaur, E.L. (2008). Differential regulation of dynein and kinesin motor proteins by Tau. Science *319*, 1086–1089.

Gebhardt, J.C., Clemen, A.E., Jaud, J., and Rief, M. (2006). Myosin-V is a mechanical ratchet. Proc. Natl. Acad. Sci. USA *103*, 8680–8685.

Gennerich, A., Carter, A.P., Reck-Peterson, S.L., and Vale, R.D. (2007). Force-induced bidirectional stepping of cytoplasmic dynein. Cell *131*, 952–965.

Gilbert, S.P., Moyer, M.L., and Johnson, K.A. (1998). Alternating site mechanism of the kinesin ATPase. Biochemistry *37*, 792–799.

Guydosh, N.R., and Block, S.M. (2006). Backsteps induced by nucleotide analogs suggest the front head of kinesin is gated by strain. Proc. Natl. Acad. Sci. USA *103*, 8054–8059.

Hackney, D.D. (1994). The rate-limiting step in microtubule-stimulated ATP hydrolysis by dimeric kinesin head domains occurs while bound to the microtubule. J. Biol. Chem. *269*, 16508–16511.

Hackney, D.D. (2005). The tethered motor domain of a kinesin-microtubule complex catalyzes reversible synthesis of bound ATP. Proc. Natl. Acad. Sci. USA *102*, 18338–18343.

Hackney, D.D. (2007). Biochemistry: processive motor movement. Science *316*, 58–59.

Hackney, D.D., Stock, M.F., Moore, J., and Patterson, R.A. (2003). Modulation of kinesin half-site ADP release and kinetic processivity by a spacer between the head groups. Biochemistry *42*, 12011–12018.

Hancock, W.O., and Howard, J. (1999). Kinesin's processivity results from mechanical and chemical coordination between the ATP hydrolysis cycles of the two motor domains. Proc. Natl. Acad. Sci. USA *96*, 13147–13152.

Hwang, W., Lang, M.J., and Karplus, M. (2008). Force generation in kinesin hinges on cover-neck bundle formation. Structure *16*, 62–71.

Kaseda, K., Higuchi, H., and Hirose, K. (2003). Alternate fast and slow stepping of a heterodimeric kinesin molecule. Nat. Cell Biol. *5*, 1079–1082.

Kawaguchi, K., and Ishiwata, S. (2001). Nucleotide-dependent single- to double-headed binding of kinesin. Science *291*, 667–669.

Kerssemakers, J.W., Munteanu, E.L., Laan, L., Noetzel, T.L., Janson, M.E., and Dogterom, M. (2006). Assembly dynamics of microtubules at molecular resolution. Nature *442*, 709–712.

Klumpp, L.M., Hoenger, A., and Gilbert, S.P. (2004). Kinesin's second step. Proc. Natl. Acad. Sci. USA *101*, 3444–3449.

Mori, T., Vale, R.D., and Tomishige, M. (2007). How kinesin waits between steps. Nature *450*, 750–754.

Ray, S., Meyhofer, E., Milligan, R.A., and Howard, J. (1993). Kinesin follows the microtubule's protofilament axis. J. Cell Biol. *121*, 1083–1093.

Reck-Peterson, S.L., Yildiz, A., Carter, A.P., Gennerich, A., Zhang, N., and Vale, R.D. (2006). Single-molecule analysis of dynein processivity and stepping behavior. Cell *126*, 335–348.

Rice, S., Cui, Y., Sindelar, C., Naber, N., Matuska, M., Vale, R., and Cooke, R. (2003). Thermodynamic properties of the kinesin neck-region docking to the catalytic core. Biophys. J. *84*, 1844–1854.

Rice, S., Lin, A.W., Safer, D., Hart, C.L., Naber, N., Carragher, B.O., Cain, S.M., Pechatnikova, E., Wilson-Kubalek, E.M., Whittaker, M., et al. (1999). A structural change in the kinesin motor protein that drives motility. Nature *402*, 778–784.

Rock, R.S., Rice, S.E., Wells, A.L., Purcell, T.J., Spudich, J.A., and Sweeney, H.L. (2001). Myosin VI is a processive motor with a large step size. Proc. Natl. Acad. Sci. USA *98*, 13655–13659.

Rosenfeld, S.S., Fordyce, P.M., Jefferson, G.M., King, P.H., and Block, S.M. (2003). Stepping and stretching: how kinesin uses internal strain to walk processively. J. Biol. Chem. *278*, 18550–18556.

Rosenfeld, S.S., Jefferson, G.M., and King, P.H. (2001). ATP reorients the neck linker of kinesin in two sequential steps. J. Biol. Chem. *276*, 40167–40174.

Schief, W.R., Clark, R.H., Crevenna, A.H., and Howard, J. (2004). Inhibition of kinesin motility by ADP and phosphate supports a hand-over-hand mechanism. Proc. Natl. Acad. Sci. USA *101*, 1183–1188.

Schief, W.R., and Howard, J. (2001). Conformational changes during kinesin motility. Curr. Opin. Cell Biol. *13*, 19–28.

Schnitzer, M.J., and Block, S.M. (1995). Statistical kinetics of processive enzymes. Cold Spring Harb. Symp. Quant. Biol. *60*, 793–802.

Schnitzer, M.J., and Block, S.M. (1997). Kinesin hydrolyses one ATP per 8-nm step. Nature *388*, 386–390.

Schuler, B., Lipman, E.A., Steinbach, P.J., Kumke, M., and Eaton, W.A. (2005). Polyproline and the "spectroscopic ruler" revisited with single-molecule fluorescence. Proc. Natl. Acad. Sci. USA *102*, 2754–2759.

Skiniotis, G., Surrey, T., Altmann, S., Gross, H., Song, Y.H., Mandelkow, E., and Hoenger, A. (2003). Nucleotide-induced conformations in the neck region of dimeric kinesin. EMBO J. *22*, 1518–1528.

Spudich, J.A. (2006). Molecular motors take tension in stride. Cell *126*, 242–244.

Svoboda, K., and Block, S.M. (1994). Force and velocity measured for single kinesin molecules. Cell *77*, 773–784.

Svoboda, K., Schmidt, C.F., Schnapp, B.J., and Block, S.M. (1993). Direct observation of kinesin stepping by optical trapping interferometry. Nature *365*, 721–727.

Thorn, K.S., Ubersax, J.A., and Vale, R.D. (2000). Engineering the processive run length of the kinesin motor. J. Cell Biol. *151*, 1093–1100.

Tomishige, M., Stuurman, N., and Vale, R.D. (2006). Single-molecule observations of neck linker conformational changes in the kinesin motor protein. Nat. Struct. Mol. Biol. *13*, 887–894.

Uemura, S., and Ishiwata, S. (2003). Loading direction regulates the affinity of ADP for kinesin. Nat. Struct. Biol. *10*, 308–311.

Vale, R.D. (2003). The molecular motor toolbox for intracellular transport. Cell *112*, 467–480.

Valentine, M.T., and Gilbert, S.P. (2007). To step or not to step? How biochemistry and mechanics influence processivity in Kinesin and Eg5. Curr. Opin. Cell Biol. *19*, 75–81.

Yildiz, A., Forkey, J.N., McKinney, S.A., Ha, T., Goldman, Y.E., and Selvin, P.R. (2003). Myosin V walks hand-over-hand: single fluorophore imaging with 1.5-nm localization. Science *300*, 2061–2065.

Yildiz, A., Tomishige, M., Vale, R.D., and Selvin, P.R. (2004). Kinesin walks hand-over-hand. Science *303*, 676–678.